Check for updates

Remediation of water contaminated with polycyclic aromatic hydrocarbons using liquid phase plasma: Influence of electrical discharge condition

Ui-Jun Kim[1], Nagahiro Saito[2,3,4,5] and Seung-Hyo Lee[1]*

[1]Division of Ocean Advanced Materials Convergence Engineering, Korea Maritime & Ocean University, Busan, South Korea, [2]Department of Chemical Systems Engineering, Graduate School of Engineering, Nagoya University, Nagoya, Japan, [3]Conjoint Research Laboratory in Nagoya University, Shinshu University, Nagoya, Japan, [4]Japan Science and Technology Corporation (JST), Open Innovation Platform with Enterprises, Research Institute and Academia (OPERA), Nagoya, Japan, [5]Japan Science and Technology Corporation (JST), Strategic International Collaborative Research Program (SICORP), Nagoya, Japan

Although the number of vessels with exhaust gas cleaning systems (EGCSs or scrubbers) has sharply increased to comply with strengthened regulations for marine environment, secondary pollutions are caused by discharged polycyclic aromatic hydrocarbons (PAHs) from scrubber effluent. Here, liquid-phase plasma (LPP) is employed to remediate water contaminated with PAHs. The increased frequency and pulse width enhanced the degradation efficiency, and 93.3, 90.7, 86.0, and 85.4% for naphthalene (Nap), acenaphthene (Ace), fluorene (Flu), and phenanthrene (Phe), respectively, are degraded at a frequency of 30 kHz and pulse width of 3 μs in 10 min. Considering physical condition of the plasma, long pulse width accelerated electrons, leading to increased generation of active species from intensified collision between electrons and surrounding molecules. Conversely, high frequency decelerated electrons due to the excessive changes in the polarity. However, the increased number of plasma discharges results in the generation of numerous active species. Generations of •OH and O radicals are confirmed by optical emission spectrometry and electron paramagnetic resonance. In addition, changes in functional groups which are corresponding to hydroxyl and oxygen groups are identified by Fourier transform infrared spectroscopy. Total PAHs in real scrubber are reduced from 1.1 to 0.4 μgL^{-1} with degradation efficiency of 63.6% after 10 min of LPP treatment. This study suggests LPP can be a promising method to protect diverse aqueous environments and provides optimal electrical discharge condition for degradation of organic pollutants.

Introduction

Polycyclic aromatic hydrocarbons (PAHs) are a large group of organic compounds with two or more benzene rings as a result of incomplete combustion from natural (e.g., forest fires, volcanic eruptions, and reactions in living beings) and anthropogenic (transportation, cooking, and industrial activities) processes. PAHs can lead to a variety of harmful effects, including bioaccumulation, carcinogenicity, genotoxicity, and endocrine disruption. The United States Environmental Protection Agency (USEPA) has categorized 16 PAHs as priority contaminants based on their potential for human exposure, toxicity, frequency of occurrence at hazardous waste sites, and information availability. The International Agency for Research on Cancer (IARC) has classified and managed some PAHs as carcinogens.

In the field of marine environment, the number of studies on the hazards of PAHs from exhaust gas cleaning system (EGCS or scrubber) effluents has recently increased (Chen et al., 2022; Ji et al., 2022; Ytreberg et al., 2022). As the International Maritime Organization (IMO) has tightened the limits of sulfur emission (MARPOL, 2008), the number of vessels with scrubbers has sharply increased from 12 in 2011 to 4047 in 2020 (ICCT website). Even though wash water contains detrimental components such as sulfate, nitrate, particulate matter, heavy metals, nutrients, and PAHs, at least 10 Gt of scrubber wash water is emitted annually without additional regulations (Osipova et al., 2021). Thor et al. (2021) observed significantly elevated mortality rates and impaired molting of pelagic copepods in 0.04% and 1% scrubber effluent which contain 2.8 and 3.8 μg/L of total hydrocarbon, respectively. In addition, Du et al. (2022) reported that the concentration of PAHs in scrubber effluent discharge could be underestimated by a factor of up to 30, and the overall marine environment impact could be further underestimated because of PAHs derivatives. Therefore, focusing on discharged PAHs from scrubber effluent and developing an efficient method to degrade PAHs in water are necessary.

Conventional processes for remediating PAH-contaminated environment are generally divided into physical, chemical, and biological treatments. Physical processes (e.g., filtration, sorption, and coagulation) can easily remove PAHs from water and soils; however, other treatments must be sequentially performed for degrading PAHs. Although chemical processes (e.g., dosage of chemical reagents, ozonation, and direct photolysis) show high removal efficiency, they require the use of chemical reagents, neutralization, and energy utilization. In addition, biological processes (e.g., phytoremediation, bacteria, and algae) require several days or even months. Advanced oxidation processes, such as Fenton reaction and photocatalysis, show great remediation performance, but additional chemical reagents or treatments are required to degrade organic pollutants.

Existing plasma technologies normally operate in soil or air conditions.

Recently, liquid-phase plasma (LPP) has been applied to the decomposition of organic pollutants in water (Baroch et al., 2008) because of its advantages, such as short treatment time, simple and compact components of setup without any chemical reagents or additional treatment, and direct discharge in water. LPP is a non-thermal plasma in solution that is conducted at room temperature under atmospheric pressure conditions. This phenomenon can be explained using the bubble theory. In principle, plasma is hardly generated in the liquid phase because electrons are collision-prone and lose electrical energy before accelerating (Saito et al., 2017). However, when a bipolar pulsed voltage is applied to the electrodes, bubbles are formed between the electrodes because of Joule heating and electrolysis (Saito et al., 2015). As the current passing through the small surface area of the electrodes provides thermal energy and electrochemical reactions, the liquid between the electrodes is heated to its boiling point and bubbles are generated. This phase change provides suitable conditions for electron avalanche. As a consequence of the generated plasma, various active species (e.g., H•, •O_2^-, H_2O_2, and •OH), high-energy electrons, and ultraviolet (UV) radiation were produced and reacted with the surrounding molecules. The detailed stages of plasma generation and electrical properties of LPP are shown in Figure S1.

As a pioneer in water remediation, LPP was innovatively employed to remediate PAH-contaminated water using plasma products. Naphthalene (Nap), acenaphthene (Ace), fluorene (Flu), and phenanthrene (Phe) were used in the experiments because of their high contents in real scrubber effluents in previous reports, and their proportions are shown in Figure S2. (Exhaust Gas Cleaning Systems Association (EGCSA) and Euroshore, 2018; Magnusson et al., 2018; Ushakov et al., 2020; Schmolke et al., 2020). The degradation performance of the LPP was evaluated under diverse pulse widths and frequencies because the characteristics of the plasma are directly influenced by the electrical discharge conditions from previous studies (Tantiplapol et al., 2015). To comprehend the plasma field and deduce the optimal electrical discharge conditions, relationships among electrical discharge conditions, physical condition of plasma and chemically active species are investigated and established. In addition, generated active species and changes in the functional groups of PAHs are identified. Finally, The performance of LPP to remediate real scrubber effluent was evaluated at the deduced electrical discharge condition.

Materials and methods

Reagents

Nap, Ace, Flu, and Phe (≥ 98%) were purchased from Sigma-Aldrich (St. Louis, MO, USA), and their physicochemical

properties are listed in Table 1. Deionized water was prepared in the laboratory using an ultrapure water machine (New Pure Power, Human Corporation, Seoul, Korea). All other organic and inorganic reagents were of analytical grade and were used as purchased without further purification.

Experimental setup

Figure 1 shows a schematic illustration of the apparatus, plasma reaction field, and products of the LPP. The experimental setup mainly comprised a bipolar pulse power supply, reactor, liquid, and electrodes. Two coaxial tungsten rod electrodes were insulated using alumina tubes that concentrated the energy on the tips and were placed inside the LPP reactor using silicon plugs. The diameter, gap, and protrusion of the electrodes were set to 1 mm. For synthetic PAHs solution, the stock solution was synthesized by adding 20 mg of PAHs to 40 mL of methanol. As mentioned above, the concentration of PAHs in scrubber effluents could be much higher than expected. Even though the solubility of PAHs in water is inferior, their actual concentrations in water have been found at levels up to 8.31 mg/L due to their adsorption on particular matter (Mojiri et al., 2019). In addition, most research on PAHs has treated on PAH_{EPA16}. However, 660 PAHs structures have been classified (Sander and Wise, 1997), and PAHs can react with atmospheric oxidants producing derivatives resulting in an increase of the actual concentrations of PAHs (Durant et al., 1996). Therefore, 1 mL of the stock solution was diluted to 10 mg/L of PAHs in 50 mL of aqueous solution. Potassium chloride (3 mM) was added to the solution for electric conductivity for generating a plasma discharge. The frequency and pulse width were varied in the range of 10–30 kHz and 1–3 μs, respectively. For real scrubber effluent sample, experiment was conducted at a frequency of 30 kHz and a pulse width of 3 μs for 10 min without any additional treatment. The solution was mixed using a magnetic stirrer (MS-300HS, Misung Scientific Co., Ltd, Seoul, Korea) to obtain a homogeneous active plasma field during the experiments. All experiments were performed at room temperature 25°C and atmospheric pressure, and were conducted thrice to ensure reproducibility.
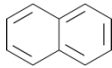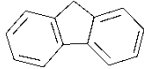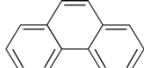
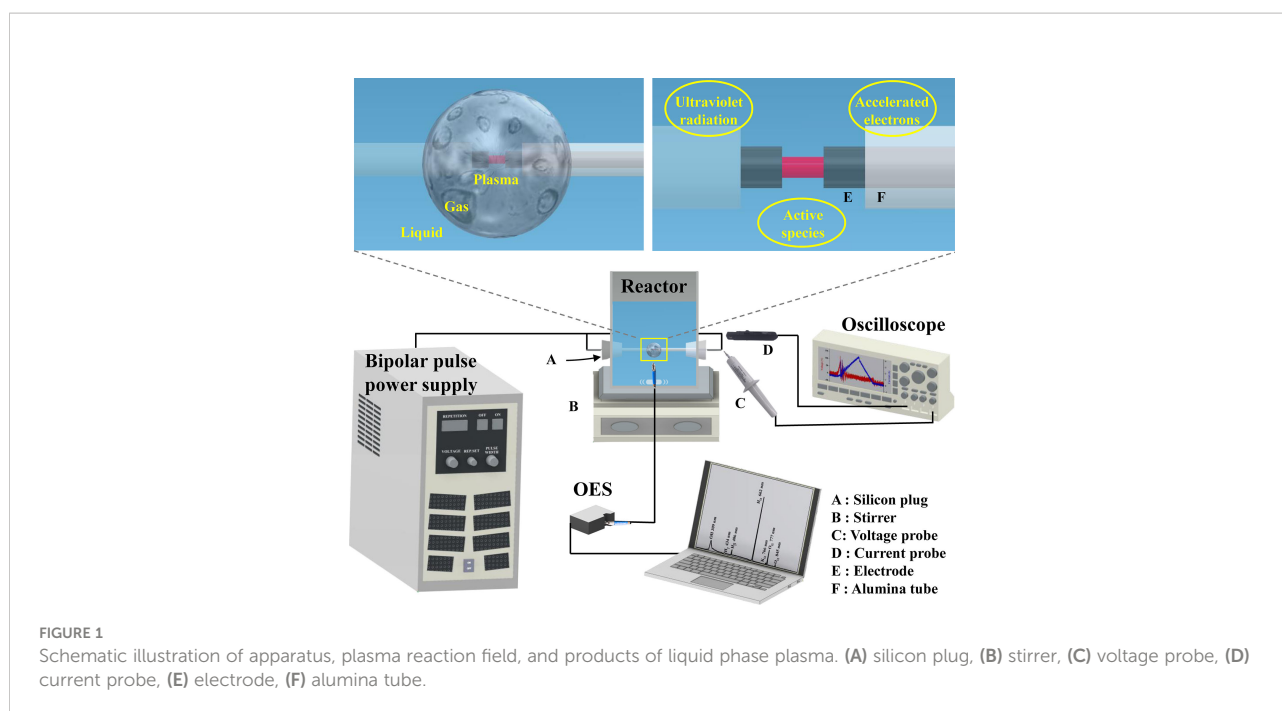## Real scrubber effluent sampling

Real scrubber effluent sample was collected from the outlet of the closed-loop scrubber. The pH and salinity of the effluent were 7.2 and 33.9 psu, respectively, but the pH was changed to 2.3 after adding a small amount of hydrogen chloride and sodium thiosulfate to deactivate biological activity and free chlorine. The samples were stored in amber glass bottles. The bottles were stored in cooler boxes during transportation to laboratory, then stored in a refrigerator at 4 °C. All samples were analyzed for less than 7 d from collection. The pH of solution was set at 7.0 by adding sodium hydroxide to set the same condition when the effluent was collected. The challenging sampling conditions restricted the amount of effluent to 2 L; therefore, the test was conducted only once.

Extraction

Samples for high-performance liquid chromatography (HPLC) and Fourier transform infrared spectroscopy (FTIR) analysis were prepared as follows: 50 mL of the treated solution from the LPP reactor was transferred into a separatory funnel with PTFE caps. Fifteen milliliters of methylene chloride was used to rinse the reactor, and the rinsed solvent was transferred to the separatory funnel. The separatory funnel was sealed and shaken for 1 min with periodic venting to release excess pressure. The mixture was allowed to equilibrate for 10 min. Subsequently, 5 mL dichloromethane was separated and dried under nitrogen. For HPLC analysis, the extract was dissolved in 2 mL of acetonitrile and filtered through PTFE filters prior to analysis. All samples were stored in brown sample vials in a refrigerator at 4°C until analysis. For the FTIR analysis, the extraction was

TABLE 1 Physical-chemical properties of selected PAHs (Mackay and Callcott, 1998).

PAHs	Abbr.	C_0 (mg/L)	Chemical Structure	Formula	Mole.Weight (g/mol)	Solubility (mg/L)	BP(°C)	MP(°C)
Naphthalene	Nap	10		$C_{10}H_8$	128.2	31.0	218.0	80.5
Acenaphthene	Ace	10		$C_{12}H_{10}$	154.2	3.8	277.5	96.2
Fluorene	Flu	10		$C_{13}H_{10}$	166.2	1.9	295.0	116.0
Phenanthrene	Phe	10		$C_{14}H_{10}$	178.2	1.1	339.0	101.0

Schematic illustration of apparatus, plasma reaction field, and products of liquid phase plasma. **(A)** silicon plug, **(B)** stirrer, **(C)** voltage probe, **(D)** current probe, **(E)** electrode, **(F)** alumina tube.

repeated thrice and then combined. The extract was dissolved in 100 µL dichloromethane and deposited in potassium bromide to obtain a pellet.

Analysis

The pH and salinity of collected scrubber effluent were measured using portable multiple water quality meter (mm-42dp, TOADKK, JAPAN). The electrical characteristics of the LPP were monitored using an oscilloscope (MSO 3014, Tektronix, Beaverton, OR, USA) equipped with a voltage probe (P6015A, Tektronix) and a current probe (TCP0020, Tektronix). HPLC (Waters e2695, Waters, Milford, MA, USA) was used to measure the concentration of PAHs in the synthetic PAHs solution, and a photodiode array detector (PDA) (2998 PDA, Waters) was used to record the absorption spectra. A Sunfire C18 column (4.6 mm × 250 mm × 5 µm, Waters) was used for separation. The mobile phase included acetonitrile (component A) and water (5% acetonitrile) as component B. Isocratic elution was performed for 5 min using acetonitrile/water (4:6) (v/v), followed by linear gradient elution to 100 acetonitrile for more than 25 min at a flow rate of 1 mL min⁻¹. Ten microliters of the samples were injected into the HPLC system using a micro syringe and detected at 220 nm for Nap and Ace and 254 nm for Flu and Phe. The ISO 28540:2011 testing method was executed for measuring the concentrations of PAH_{EPA16} in real scrubber effluent by the Korea Testing & Research Institute in Busan, Korea. The reports associated with this are No. TAK-2022-083818 and No. TAK-2022-098074 and

GC-MS instruments (7010 B, Agilent, Santa Clara, CA, USA) were used. FTIR (iS50, Thermo Fisher Scientific, Waltham, MA, USA) was used to characterize the chemical bonds of the samples. The transmittance mode was used, and the spectra were obtained from 400–4,000 cm⁻¹ with a resolution of 1 cm⁻¹. The reactive species were identified using optical emission spectrometry (OES) (FLAME-T-XR1, Ocean Insight, Orlando, FL, USA) and electron paramagnetic resonance (EPR) spectrometry. Electron paramagnetic resonance (EPR, EMX Plus, Bruker, Billerica, MA, USA) was measured at a microwave frequency of 9.425 GHz. For EPR analysis, 5',5-dimethyl-1-pyrroline N-oxide (DMPO) and 2,2,6,6-tetramethylpiperidine (TEMP) were added to the solution as spin-trapping reagents.

Data processing

The degradation efficiency (η) and degradation rate constant (k) were calculated using the following equations.

$$\eta \ (\%) = \frac{C_0 - C_t}{C_0} \times 100$$

$$\ln\left(\frac{C_0}{C_t}\right) = kt$$

where t is the LPP treatment time, C_o is the initial concentration of PAHs in the aqueous solution, C_t is the concentration of PAHs in the solution treated with LPP for t in, and k is the rate constant (min⁻¹).

The energy yield was calculated using the following equation.

$$Y = \frac{C_0 \times V \times \eta}{P \times t}$$

where Y is the energy yield (g/kW•h), C_os the initial concentration of PAHs (g/L), V is the volume of the reaction liquid (L), η is the removal efficiency of PAHs (%), P is the power consumed during discharge (kW), and t is the reaction time (h). The units were converted to mg/kJ.

The electron temperature can be calculated from the relative intensities of the spectral lines of excited hydrogen H_β to H_α assuming a quasi-local thermodynamic equilibrium in the LPP, using the following equation (Lochte-Holtgreven, 1998):

$$\frac{I_\beta}{I_\alpha} = \frac{A_\beta g_\beta \lambda_\alpha}{A_\alpha g_\alpha \lambda_\beta} exp\left\{-\frac{E_\beta - E_\alpha}{kT}\right\}$$

where I, A, g, λ, E, k and T represent the emission intensity of H radicals from OES data, the transition probability or Einstein coefficient (s^{-1}), statistical weight, wavelength (m), upper level energy (J), Boltzmann constant (1.38×0^{-23} J/K), and electron temperature (K), respectively.

Results and discussion

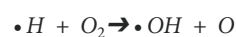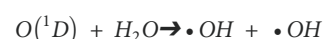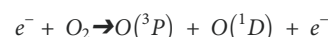## Performance of liquid phase plasma on remediation of synthetic PAHs solution

Figure 2 shows the concentrations of PAHs after 10 min of LPP treatment at different frequencies from 10–30 kHz and pulse widths from 1–3 μs. The degradation efficiencies of Nap, Ace, Flu, and Phe were 53.2, 45.9, 35.7, and 34.3%, respectively, at a frequency of 10 kHz and pulse width of 1 μs. Conversely, the highest degradation efficiencies of Nap, Ace, Flu, and Phe were 93.3, 90.7, 86.0, and 85.4%, respectively, at a frequency of 30 kHz and a pulse width of 3 μs. The numerical values for each PAHs are presented in Table S1. Those values show rapid degradation of PAHs in water was achieved by LPP comparing with previous studies as shown in Table S2.

Moreover, the degradation kinetics and energy efficiencies were evaluated under the optimum electrical discharge conditions. As shown in Figure 3A, four curves were well fitted with the pseudo-first-order reaction equation well (R-square: 0.990, 0.994, 0.934, and 0.937). The rate constant of Nap degradation was the highest (0.259 min^{-1}), and that of Phe degradation was the lowest (0.173 min^{-1}). The rate constants of PAHs degradation decrease with increasing molecular weight. These results are in accordance with earlier studies that showed higher degradation efficiency with lower molecular weight PAHs than with higher molecular weight PAHs (Lei et al., 2007; Li et al., 2014). It is known that higher-molecular-weight PAHs are poorly degraded because of their higher volatility and solubility.

Furthermore, the energy yield decreased with increasing molecular weight (Figure 3B). The highest energy yields obtained for Nap, Ace, Flu, and Phe were 0.0550, 0.0455, 0.0409, and 0.0372 mg/kJ with 2 min of treatment time. These values are higher than those of previous studies (0.008 (Abbas et al., 2020A), 0.012 (Li et al., 2016), and 0.019 mg/kJ (Abbas et al., 2020B)). The lowest energy yields obtained for Nap, Ace, Flu, and Phe were 0.0200, 0.0195, 0.0185, and 0.0183 mg/kJ, respectively, after 10 min of treatment. These results are caused by the lower reactions between PAHs and active species due to the lower concentrations of PAHs. The degradation efficiencies and energy yields of Nap, Ace, Flu, and Phe are presented in Table S3.

Role of active species generated from liquid phase plasma

Optical diagnostics were performed using OES for identifying the active species during plasma treatment. Figure 4 shows the optical emission spectrum of LPP in the range of 200–1,050 nm. The major active species were atomic hydrogen (λ = 656 nm), atomic oxygen ($3p^5P \rightarrow 3s^5S^0$ at λ = 777 nm), and hydroxyl radicals ($A^2\Sigma^+ \rightarrow X^2\Pi$ at λ = 309 nm). The observed radicals were generated by collisions between electrons and surrounding molecules, and the reactions are shown below (Chokradjaroen et al., 2021):

$$e^- + H_2O \rightarrow \bullet OH + \bullet H + e^-$$

$$e^- + O_2 \rightarrow O(^3P) + O(^1D) + e^-$$

$$O(^1D) + H_2O \rightarrow \bullet OH + \bullet OH$$

$$\bullet H + O_2 \rightarrow \bullet OH + O$$

$$O + O \rightarrow O_2$$

Furthermore, these active species participated in subsequent reactions with active species, UV radiation, or other physical-chemical products from the plasma, producing •OH, O•, O_3, H_2O_2, and O_2H• and their oxidation potentials are shown in Table S4. The dependence of the optical emission spectrum on the electrical discharge conditions is shown in Figure S3.

The FTIR spectrum provides qualitative and quantitative information regarding the functional groups and chemical bonds of PAHs by evaluating the specific absorption resulting from changes in the dipole moment of the molecules. Therefore, FTIR analysis was performed to discover active species which give significant influences on degradation of PAHs. Figure 5 shows the significantly changed FTIR spectra after liquid-phase plasma treatment at a frequency of 30 kHz and pulse width of 3 μs. The range of 600–900 cm^{-1} is characteristic of the number of
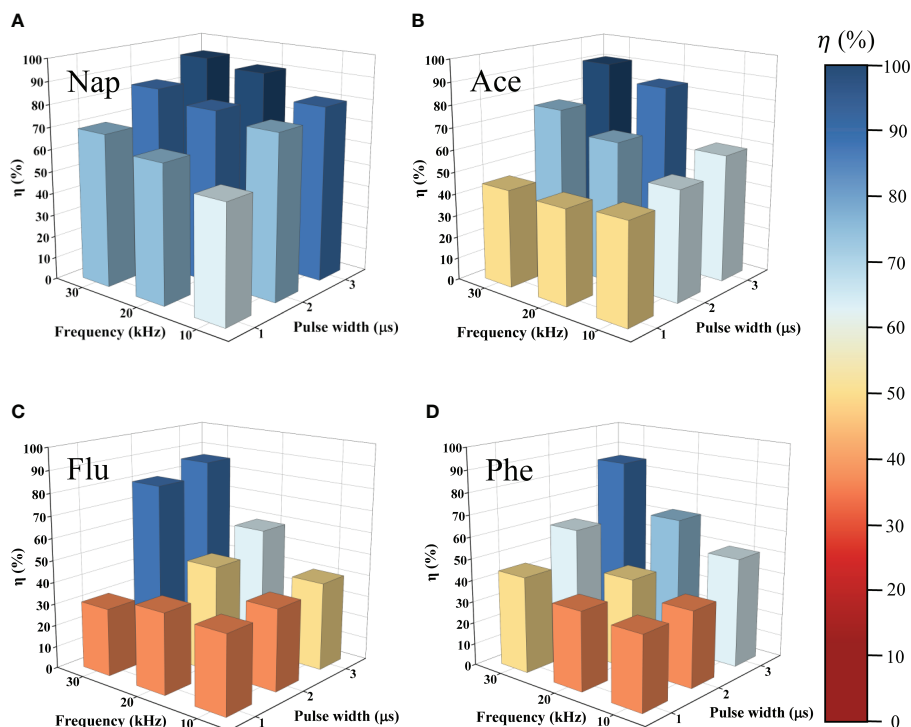
FIGURE 2
Degradation efficiency of **(A)** Nap, **(B)** Ace, **(C)** Flu, and **(D)** Phe as function of applied frequency and pulse width after 10 min in liquid phase plasma process. Degradation efficiency increased with increased frequency and pulse width.

adjacent hydrogen atoms on the aromatic ring, and the peaks at 781, 784, 737, and 733 cm^{-1} in Figure 5, which correspond to Nap, Ace, Flu, and Phe, respectively, declined or almost disappeared after 10 min, indicating PAH degradation (Socrates, 2004). Considering that the reduction of the peaks at 781 cm^{-1} in Figure 5A and 784 cm^{-1} in Figure 5B were larger

than those at 737 cm^{-1} in Figure 5C and 733 cm^{-1} in Figure 5D, FTIR showed a correlation between the degradation efficiency and the molecular weight of PAHs which is the same as HPLC results presented. In addition, while the aromatic C-H stretching peak at 3,054 cm^{-1} decreased, the aliphatic C-H stretching peaks at 2,853 cm^{-1}, 2,925 cm^{-1}, and 2,957 cm^{-1} increased, indicating
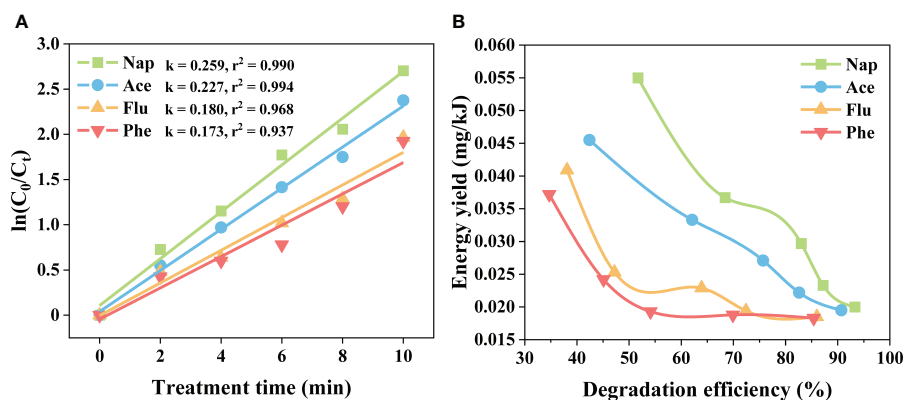

FIGURE 3
(A) Degradation kinetics and **(B)** energy efficiencies of Nap, Ace, Flu, and Phe at a frequency of 30 kHz and a pulse width of 3 μs. Both nearly decreased with increased molecular weight.
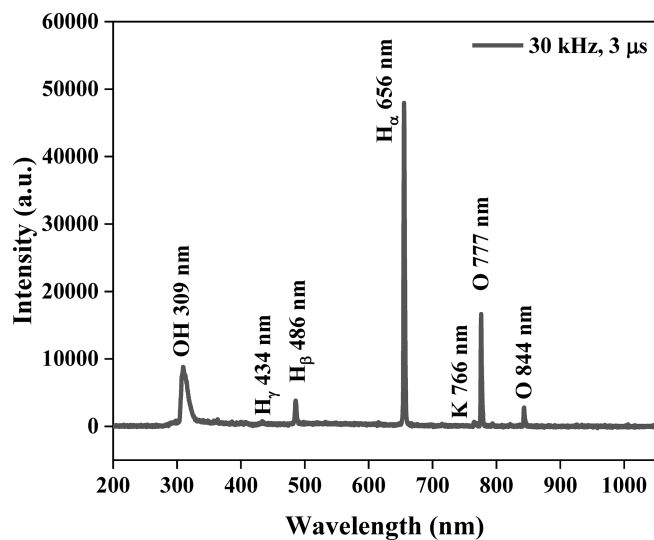
FIGURE 4
Identification of active species from liquid phase plasma in deionized water including 3 mM KCl by optical emission spectrometer at a frequency of 30 kHz and a pulse width of 3 µs. The major active species were atomic hydrogen (λ = 656 nm), atomic oxygen (λ = 777 nm), and hydroxyl radicals (λ = 309 nm).
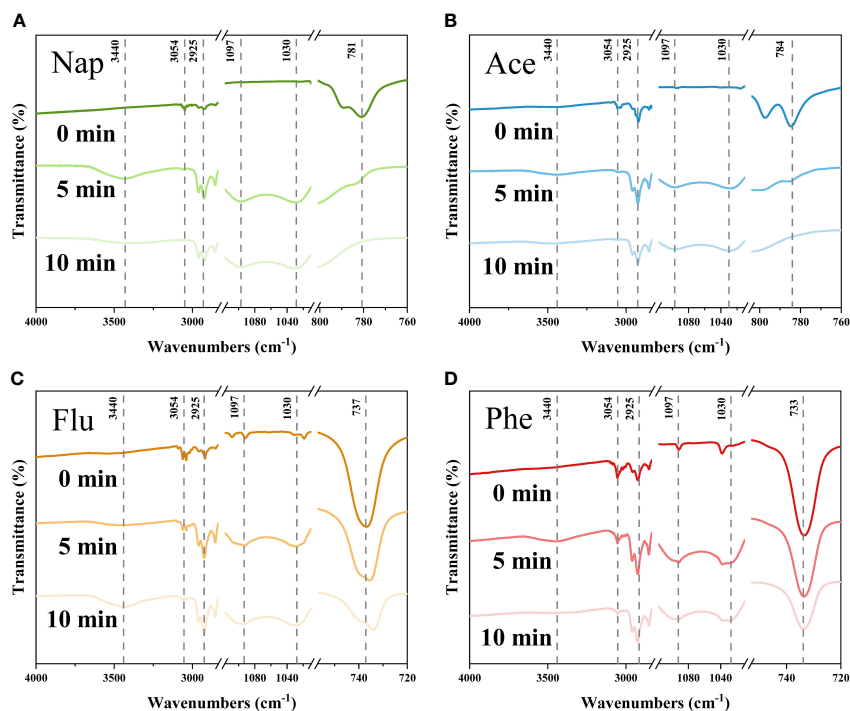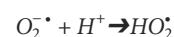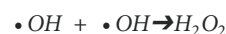

FIGURE 5
FTIR spectra of **(A)** Nap, **(B)** Ace, **(C)** Flu, and **(D)** Phe before and after the liquid phase plasma treatment. The characteristic peaks of PAHs in the range between 600−900 cm^{-1} decreased. Moreover, hydroxyl and oxygen groups are formed after the treatment in the region of 3,160−3,600 cm^{-1} and 1,000−1,260 cm^{-1}, respectively.

that the rings of PAHs were opened (Skoog et al., 2017). In particular, the band centered at 3,440 cm^{-1} increased after plasma treatment, corresponding to the O-H stretching vibration from hydroxyl groups, and peaks in the region of 1,260–1,000 cm^{-1} were formed, which are correlated with C-O stretching vibration from alcohol, ethers, carboxylic acids, or ester stretching vibrations (Mangun et al., 2001).

The formation of hydroxyl and oxygen functional groups after the LPP treatment and the observation of •OH and O radicals from OES analysis suggest that •OH and O radicals participate in PAHs oxidation and give significant influences on degradation of PAHs. *via* This is in good agreement with observations of previous studies on plasma treatments which state that the aromatic ring can be primarily attacked by •OH presenting byproducts using gas chromatography equipped with mass detector (Abbas et al., 2020B), and show their oxidation potentials, as shown in Table S4. In addition, advanced oxidation processes (AOPs) (Yang et al., 2018), such as photocatalysis, Fenton reactions (Ke et al., 2018), and hybrid technologies that combine different processes (Wu et al., 2018) aimed at the decomposition of organic pollutants through reactions with •OH, have been applied to remediate PAH-contaminated soil and water.

In our study, increased frequency and pulse width improved the degradation efficiency. In addition, the generation of •OH and O radicals and their participation in PAH oxidation were confirmed by OES and FTIR analyses. As active species are fundamentally generated through electron impact dissociation (Mai-Prochnow et al., 2021), the determination of the electron temperature is important for understanding and optimizing LPP. However, there is hardly any specific plasma state in numerous studies on degradation of organic pollutants using plasma technology comparing degradation efficiency varying electrical discharge conditions (Li et al., 2016; Zhan et al., 2018; Lu et al., 2022). Therefore, we calculated electron temperature and compared it to electrical discharge conditions; active species as shown in Figures 6A, B. Phe was chosen as a representative PAHs owing to its low degradation efficiency. To show the number of generated radicals, the optical emission intensity of the •OH is shown in Figure 6A, and that of the O radical is shown in Figure 6B. The calculated and detected values are listed in Table S2. Given that the behaviors of the optical emission of •OH and O radicals were nearly in accordance with that of the degradation efficiency, they extensively contributed to the degradation of PAHs. In particular, the •OH showed the most similar behavior to Phe degradation efficiency. This may be due to the higher oxidation potential of •OH compared to that of O radicals. The input energy increased with an increase in the pulse width (Table S2), and then, more accelerated electrons led to intensified interactions with the surrounding molecules, generating •OH and O radicals. In contrast, the electron temperature decreased with increased frequency. It is assumed that the change in the

polarity of the electrode is fast enough such that the electrons see a reversal in the field before reaching the electrode and oscillate between the two electrodes (Dhali, 2020). However, the increased number of plasma discharges results in the generation of numerous active species. The mechanism by which LPP degrades PAHs is depicted with contrasting pulse widths and frequencies for an explicit description in Figure 6C and Figure 6D. A longer pulse width and higher frequency lead to more accelerated electrons and frequent bombardment between the electrons and water, resulting in the generation of more active species that degrade organic pollutants. Based on this mechanism, optimal performance could be achieved by increasing the pulse width and frequency. In a few cases, the degradation efficiency is not exactly proportional to the optical emission of the •OH and O radicals. This is probably due to interactions among the active species, and the conversion of the produced species can be represented as follows (Evans and Goldfine, 2000; Chen et al., 2004):

$$\bullet OH + \bullet OH \rightarrow H_2O_2$$

$$O_2^{-\bullet} + H^+ \rightarrow HO_2^{\bullet}$$

$$O_2^{-\bullet} + H_2O_2 \rightarrow O_2 + HO_2^{\bullet} + \bullet OH$$

To quantitatively compare the amount of generated •OH and confirm the involvement of •OH and O radicals in the oxidation reactions, they were trapped with DMPO and TEMP. Figures 7A and 7B exhibit typical spectra of DMPO-hydroxyl radical adducts with a 1:2:2:1 quartet characteristic. As shown in Figure 7A, the amplitude of the DMPO-hydroxyl radical signal increased with increasing treatment time, and the highest values at treatment times of 2, 6, and 10 min were 1,684, 3,881, and 5,191, respectively. Methanol is known as one of the most efficient hydroxyl radical scavengers and was used in stock solutions in this study. The results of the EPR analysis in Figure 7B verify the effectiveness of •OH in participating in chemical reactions, even in the presence of methanol. It is assumed that when LPP is adopted to remediate real wastewater in the absence of a hydroxyl radical scavenger, enhanced performance would be achieved. Figure 7C shows a typical spectrum of TEMP-oxygen radical adducts with a 1:1:1 triplet characteristic. As with the OES results, which observed O radicals, and FTIR results, which proved its participation in the oxidation of PAHs, the EPR results also continuously proved that O radicals were produced and oxidized organic pollutants.

Application for real scrubber effluent

Though studies on the harmful effects and analysis of PAHs in scrubber effluent have been recently introduced, a suitable process to degrade them remains undeveloped yet (Thor et al., 2021; Chen
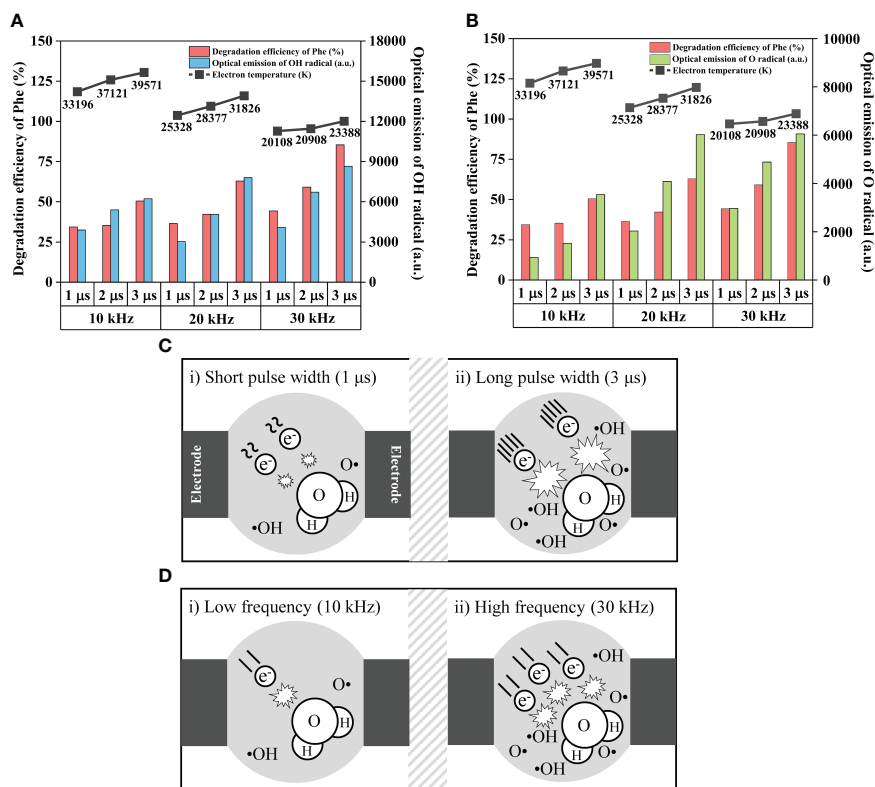
FIGURE 6
Graphical behaviors of electrical discharge conditions, electron temperature, the degradation efficiency of Phe, and the optical emission intensity of **(A)** hydroxyl radical, and **(B)** oxygen radical. Mechanism of liquid phase plasma to degrade PAHs with contrasting **(C)** pulse widths and **(D)** frequencies. Hydroxyl radical showed the most similar behaviors to the degradation efficiency. Increased pulse widths and frequencies lead to more accelerated electrons and frequent bombardment between electron and surrounding molecule, resulting in increased generation of active species which oxidize PAHs.

et al., 2022; Ji et al., 2022). Therefore, LPP was employed to degrade PAHs in real scrubber effluent and the performance was assessed. The treated effluent was analyzed after 10 min of treatment at a frequency of 30 kHz and pulse width of 3 μs. Figure 8 shows the

results, and each concentration is listed in Table S5. Total PAH_{EPA16} were reduced from 1.1 to 0.4 μg/L with degradation efficiency of 63.6%. It is particularly remarkable that high molecular weight PAHs (HMW-PAHs) which consist of four or
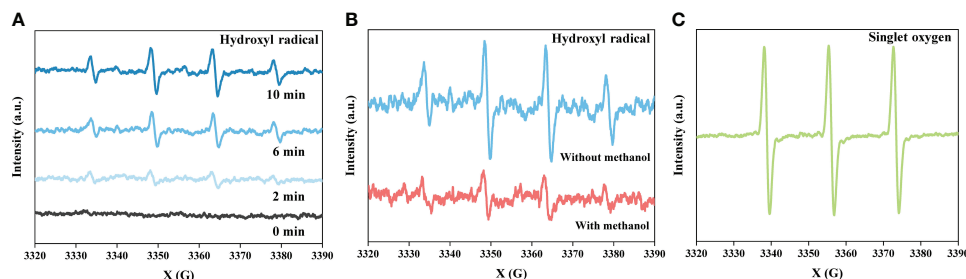
FIGURE 7
(A) EPR spectra of DMPO-hydroxyl radical adducts as a function of treatment time, **(B)** the spectra from with or without methanol contained water, and **(C)** the spectrum of TEMP-oxygen radical adducts at a frequency of 20 kHz and a pulse width of 2 μs. This shows quantitative comparison of the amount of hydroxyl radical and a possibility to achieve enhanced performance of liquid phase plasma in real wastewater which has no scavengers. Contribution of oxygen radical to oxidation was also verified.

FIGURE 8
Concentration of PAH$_{EAP16}$ in real scrubber effluent before and after 10 min of the LPP treatment at a frequency of 30 kHz and a pulse width 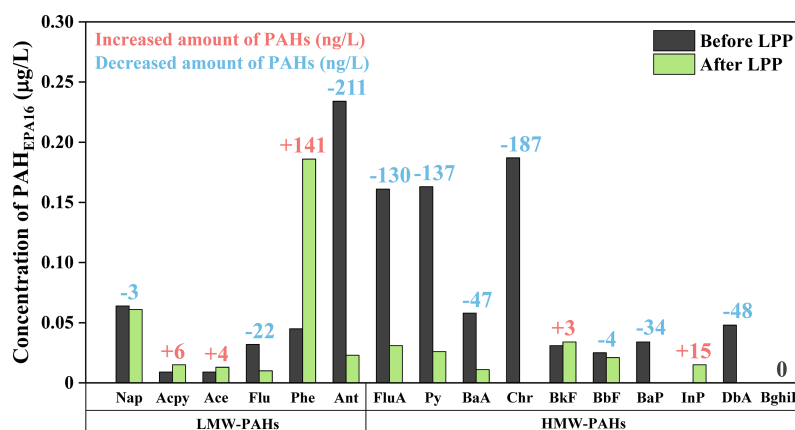of 3 μs. Although a little amount of low molecular weight PAHs (LMW-PAHs) were produced due to incomplete combustion of PAHs or their byproducts, LPP showed great performance in degradation of high molecular weight PAHs (HMW-PAHs).

more aromatic rings were effectively degraded from 0.707 to 0.138 μg/L. In contrast, the concentration of some low molecular weight PAHs (LMW-PAHs), which are composed of two or three aromatic rings, slightly decreased or increased after LPP treatment and the total amount of LMW-PAHs were reduced from 0.393 to 0.308 μg/L. It is assumed that LMW-PAHs were generated from incomplete combustion of HMW-PAHs, organic matter, and their byproducts by plasma which worked as a pyrogenic source, similar to the defined source of PAHs (Rubio-Clemente et al., 2014; Mojiri et al., 2019; Patel et al., 2020). Especially, diverse organic matter could exist in scrubber effluent because the effluent was used to treat exhaust gas. Based on our study, the generated LMW-PAHs would be degraded with a marginally extended treatment time. Although real scrubber effluent contains not only PAH$_{EPA16}$ but also substituted PAHs, other parent PAHs, heavy metals, and nutrients, LPP undergoes rapid degradation of PAHs. The benefits of LPP, such as remarkable degradation performance, simple *in situ* and compact components of setup, and direct discharge in water, might also remediate diverse industrial, pesticidal, and pharmaceutical wastewater.

Conclusions

Remediation of water contaminated by PAHs using LPP was investigated and optimal electrical discharge condition was suggested based on the physical condition of plasma. The main findings may be summarized as follows:

1. The performance of LPP was evaluated under various electrical discharge conditions. The increased pulse width and frequency improved the degradation efficiency, and the highest degradation efficiencies of Nap, Ace, Flu, and Phe were 93.3, 90.7, 86.0, and 85.4%, respectively, in 10 min at a frequency of 30 kHz and a pulse width of 3 μs.

2. OH and O radicals have been discovered to be crucial active species in the degradation of PAHs. The generation of •OH and O radicals was confirmed by optical diagnostics, and their participation in the degradation of PAHs was confirmed by the formation of hydroxyl and oxygen groups in the byproducts.

3. The effect of electrical discharge condition on the generation of chemically active species was explained by presenting the physical condition of plasma. The rapid degradation of PAHs at a long pulse width and high frequency could be achieved because of the more accelerated electrons and frequent bombardment among electrons and surrounding molecules, generating more •OH and O radicals that degrade organic pollutants.

4. The effectiveness of •OH in the presence of its scavenger was verified by EPR. LPP may achieve an enhanced performance in dealing with organic pollutants in the absence of scavengers.

5. 63.6% of PAHs in real scrubber effluent was successfully degraded by LPP at the optimal condition in 10 min without any additional treatments or chemical reagents. Given that the rapid degradation of PAHs compared to traditional methods and the direct degradation of organic pollutants in water by plasma treatment were performed, LPP provides a novel method to protect diverse aqueous environments.

Data availability statement

The original contributions presented in the study are included in the article/Supplementary Material. Further inquiries can be directed to the corresponding author.

Author contributions

U-JK: Investigation, data curation, writing-original draft preparation, methodology. NS: Conceptualization. S-HL: Supervision, validation, writing review and editing. All authors contributed to the article and approved the submitted version.

Acknowledgments

Conflict of interest

Author NS was employed by Japan Science and Technology Corporation JST.

The remaining authors declare that the research was conducted in the absence of any commercial or financial relationships that could be construed as a potential conflict of interest.

Publisher's note

All claims expressed in this article are solely those of the authors and do not necessarily represent those of their affiliated organizations, or those of the publisher, the editors and the reviewers. Any product that may be evaluated in this article, or claim that may be made by its manufacturer, is not guaranteed or endorsed by the publisher.

Supplementary material

The Supplementary Material for this article can be found online at: https://www.frontiersin.org/articles/10.3389/fmars.2022.1033962/full#supplementary-material

References

Abbas, Y., Lu, W., Dai, H., Fu, X., Ye, R., and Wang, H. (2020B). Remediation of polycyclic aromatic hydrocarbons (PAHs) contaminated soil with double dielectric barrier discharge plasma technology: Influencing parameters. *Chem. Eng. J.* 394, 124858. doi: 10.1016/j.cej.2020.124858

Abbas, Y., Lu, W., Wang, Q., Dai, H., Liu, Y., Fu, X., et al. (2020A). Remediation of pyrene contaminated soil by double dielectric barrier discharge plasma technology: Performance optimization and evaluation. *Environ. pollut.* 260, 113944. doi: 10.1016/j.envpol.2020.113944

Baroch, P., Anita, V., Saito, N., and Takai, O. (2008). Bipolar pulsed electrical discharge for decomposition of organic compounds in water. *J. Electrostat.* 66, 294–299. doi: 10.1016/j.elstat.2008.01.010

Chen, C. F., Lim, Y. C., Ju, Y. R., Albarico, F. P. J. B., Cheng, J. W., Chen, C. W., et al. (2022). Method development for low-concentration PAHs analysis in seawater to evaluate the impact of ship scrubber washwater effluents. *Water* 14 (3), 287. doi: 10.3390/w14030287

Chen, Y. S., Zhang, X. S., Dai, Y. C., and Yuan, W. K. (2004). Pulsed high-voltage discharge plasma for degradation of phenol in aqueous solution. *Sep. Purif. Technol.* 34, 5–12. doi: 10.1016/S1383-5866(03)00169-2

Chokradjaroen, C., Niu, J., Panomsuwan, G., and Saito, N. (2021). Insight on solution plasma in aqueous solution and their application in modification of chitin and chitosan. *Int. J.Mol. Sci.* 22, 4308. doi: 10.3390/ijms22094308

Dhali, S. K. (2020). Generation of large-volume high-pressure plasma by spatiotemporal control of space charge. *AIP Adv.* 10, 035002. doi: 10.1063/1.5143923

Durant, J. L., Busby, W. F.Jr., Lafleur, A. L., Penman, B. W., and Crespi, C. L. (1996). Human cell mutagenicity of oxygenated, nitrated and unsubstituted polycyclic aromatic hydrocarbons associated with urban aerosols. *Mutat. Research/Genetic Toxicol.* 371, 123–157. doi: 10.1016/S0165-1218(96)90103-2

Du, L., Zhang, L., Liu, R., and Gu, Y. (2022). Is polycyclic aromatic hydrocarbon concentration significantly underestimated in scrubber effluent discharge? *Ocean Coast. Manage.* 220, 106093. doi: 10.1016/j.ocecoaman.2022.106093

Exhaust Gas Cleaning Systems Association (EGCSA) and Euroshore (2018). Report on analyses of water samples from exhaust gas cleaning systems. *Marine Environment Protection Committee Session 73*. Available at: https://www.egcsa.com/wp-content/uploads/MEPC-73-INF.5-Study-report-on-analyses-of-water-samples-from-exhaust-gas-cleaning-systems-CESA.pdf.

Evans, J. L., and Goldfine, I. D. (2000). α-lipoic acid: a multifunctional antioxidant that improves insulin sensitivity in patients with type 2 diabetes. *Diabetes Technol. Ther.* 2, 401–413. doi: 10.1089/15209150050194279

Ji, Z., Yang, Y., Zhu, Y., Ling, Y., Ren, D., Huo, Z., et al. (2022). Toxic effects on dunaliella salina, mysidopsis bahia, and mugilogobius chulae from ship exhaust gas closed-loop scrubber wash water. *Res. Square* 1. doi: 10.21203/rs.3.rs-1324578/v1

Ke, Y., Ning, X. A., Liang, J., Zou, H., Sun, J., Cai, H., et al. (2018). Sludge treatment by integrated ultrasound-fenton process: characterization of sludge organic matter and its impact on PAHs removal. *J. Hazard. Mater.* 343, 191–199. doi: 10.1016/j.jhazmat.2017.09.030

Lei, A. P., Hu, Z. L., Wong, Y. S., and Tam, N. F. Y. (2007). Removal of fluoranthene and pyrene by different microalgal species. *Bioresour. Technol.* 98, 273–280. doi: 10.1016/j.biortech.2006.01.012

Li, R., Liu, Y., Cheng, W., Zhang, W., Xue, G., and Ognier, S. (2016). Study on remediation of phenanthrene contaminated soil by pulsed dielectric barrier discharge plasma: the role of active species. *Chem. Eng. J.* 296, 132–140. doi: 10.1016/j.cej.2016.03.054

Li, H., Qu, R., Li, C., Guo, W., Han, X., He, F., et al. (2014). Selective removal of polycyclic aromatic hydrocarbons (PAHs) from soil washing effluents using biochars produced at different pyrolytic temperatures. *Bioresour. Technol.* 163, 193–198. doi: 10.1016/j.biortech.2014.04.042

Lochte-Holtgreven, W. (1998). *Plasma diagnostics* (New York: American Institute of Physics).

Lu, H., Deng, C., Yu, Z., Zhang, D., Li, W., Huang, J., et al. (2022). Synergistic degradation of fluorene in soil by dielectric barrier discharge plasma combined with P25/NH2-MIL-125 (Ti). *Chemosphere.* 296, 133950. doi: 10.1016/j.chemosphere.2022.133950

Mackay, D., and Callcott, D. (1998). "Partitioning and physical chemical properties of PAHs," in *PAHs and related compounds* (Berlin, Heidelberg: Springer), 325–345.

Magnusson, K., Thor, P., and Granberg, M. (2018). Risk assessment of marine exhaust gas EGCS water, task 2, activity 3, EGCSs closing the loop. *IVL Swedish Environ. Res. Institute.*, 1–44.

Mai-Prochnow, A., Zhou, R., Zhang, T., Ostrikov, K. K., Mugunthan, S., Rice, S. A., et al. (2021). Interactions of plasma-activated water with biofilms: inactivation, dispersal effects and mechanisms of action. *NPJ Biofilms Microbiomes.* 7, 1–12. doi: 10.1038/s41522-020-00180-6

Mangun, C. L., Benak, K. R., Economy, J., and Foster, K. L. (2001). Surface chemistry, pore sizes and adsorption properties of activated carbon fibers and precursors treated with ammonia. *Carbon* 39, 1809–1820. doi: 10.1016/S0008-6223(00)00319-5

MARPOL (2008). Amendments to the annex of protocol of 1997 to amend the international con- vention for the prevention of pollution from ships 1973, as modified by the protocol of 1978. *(Marine Environment Protection Committee Resolution MEPC)* 176 (58)

Mojiri, A., Zhou, J. L., Ohashi, A., Ozaki, N., and Kindaichi, T. (2019). Comprehensive review of polycyclic aromatic hydrocarbons in water sources, their effects and treatments. *Sci. total Environ.* 696, 133971. doi: 10.1016/j.scitotenv.2019.133971

Osipova, L. I. U. D. M. I. L. A., Georgeff, E. L. I. S. E., and Comer, B. R. Y. A. N. (2021). Global scrubber washwater discharges under IMO's 2020 fuel sulfur limit. *Int. Counc. Clean Transp*, 10–12.

Patel, A. B., Shaikh, S., Jain, K. R., Desai, C., and Madamwar, D. (2020). Polycyclic aromatic hydrocarbons: sources, toxicity, and remediation approaches. *Front. Microbiol.* 11. doi: 10.3389/fmicb.2020.562813

Rubio-Clemente, A., Torres-Palma, R. A., and Peñuela, G. A. (2014). Removal of polycyclic aromatic hydrocarbons in aqueous environment by chemical treatments: a review. *Sci. total Environ.* 478, 201–225. doi: 10.1016/j.scitotenv.2013.12.126

Saito, N., Bratescu, M. A., and Hashimi, K. (2017). Solution plasma: A new reaction field for nanomaterials synthesis. *Jpn. J. Appl. Phys* 57 (1), 0102A4. doi: 10.7567/JJAP.57.0102A4

Saito, G., Nakasugi, Y., and Akiyama., T. (2015). Generation of solution plasma over a large electrode surface area. *J. Appl. Phy.*, 118. doi: 10.1063/1.4926493

Sander, L. C., and Wise, S. A. (1997). *Polycyclic aromatic hydrocarbon structure index NIST special publication 922* (Washington: U.S. Government Printing Office).

Schmolke, S., Ewert, K., Kaste, M., Schöngaßner, T., Kirchgeorg, T., and Marin-Enriquez, O. (2020). *Environ-mental protection in maritime traffic – scrubber wash water survey. final report* (Umweltbundesamt, Germany: German Environment Agency), 1–97. UBA Texte. Des- sau-Roßlau. Texte 162/2020.

Skoog, D. A., Holler, F. J., and Crouch, S. R. (2017). *Principles of instrumental analysis* (Boston: Cengage learning).

Socrates, G. (2004). *Infrared and raman characteristic group frequencies: tables and charts* (Chichester: John Wiley & Sons).

Tantiplapol, T., Singsawat, Y., Narongsil, N., Damrongsakkul, S., Saito, N., and Prasertsung, I. (2015). Influences of solution plasma conditions on degradation rate and properties of chitosan. *Innov. Food Sci. Emerg. Technol.* 32, 116–120. doi: 10.1016/j.ifset.2015.09.014

Thor, P., Granberg, M. E., Winnes, H., and Magnusson, K. (2021). Severe toxic effects on pelagic copepods from maritime exhaust gas scrubber effluents. *Environ. Sci. Technol.* 55, 5826–5835. doi: 10.1021/acs.est.0c07805

Ushakov, S., Stenersen, D., Einang, P. M., and Ask, T.Ø. (2020). Meeting future emission regulation at sea by combining low-pressure EGR and seawater scrubbing. *J. Mar. Sci. Technol.* 25 (2), 482–497. doi: 10.1007/s00773-019-00655-y

Wu, Z., Zhu, Z., Hao, X., Zhou, W., Han, J., Tang, X., et al. (2018). Enhanced oxidation of naphthalene using plasma activation of TiO2/diatomite catalyst. *J. Hazard Mater* 347, 48–57. doi: 10.1016/j.jhazmat.2017.12.052

Yang, X., Cai, H., Bao, M., Yu, J., Lu, J., and Li, Y. (2018). Insight into the highly efficient degradation of PAHs in water over graphene oxide/Ag3PO4 composites under visible light irradiation. *Che. Eng. J.* 334, 355–376. doi: 10.1016/j.cej.2017.09.104

Ytreberg, E., Hansson, K., Hermansson, A. L., Parsmo, R., Lagerström, M., Jalkanen, J. P., et al. (2022). Metal and PAH loads from ships and boats, relative other sources, in the Baltic Sea. *Mar. pollut. Bull.* 182, 113904. doi: 10.1016/j.marpolbul.2022.113904

Zhan, J., Liu, Y., Cheng, W., Zhang, A., Li, R., Li, X., et al. (2018). Remediation of soil contaminated by fluorene using needle-plate pulsed corona discharge plasma. *Che. Eng. J.* 334, 2124–2133. doi: 10.1016/j.cej.2017.11.093